# Damping Measurements on a Multi-Blade Cascade with Multiple Degrees of Freedom: A Francis-99 Test Case

IOP Conf. Series: Journal of Physics: Conf. Series **1296** (2019) 012003 doi:10.1088/1742-6596/1296/1/012003

# Damping Measurements on a Multi-Blade Cascade with Multiple Degrees of Freedom: A Francis-99 Test Case

**C W Bergan[1], E O Tengs[1,2], B W Solemslie [1], P Østby [1,3], and O G Dahlhaug[1]**

[1] NTNU Vannkraftlaboratoriet, 7491 Trondheim
[2] EDR & Medeso AS, NO-1337 Sandvika
[3] Rainpower AS, NO-2027 Kjeller

E-mail: carl.w.bergan@ntnu.no

**Abstract.** Due to thinner blades and higher demands for flexibility, the high-head Francis runners designed today face considerable challenges that severely affect the runners' expected lifetime. For many high-head Francis runners, the leading cause of fatigue is blade cracking due to Rotor-Stator Interaction, which cause vibrations in the runner blades.

Accurate prediction of the vibration magnitudes in a turbine is paramount in designing a reliable Francis runner. The understanding of the interaction between the hydrodynamic forces and the internal stresses in the runner is not yet sufficient to make this prediction. Previous investigations have identified some key parameters that affect dynamic behaviour in water, such as added mass, as well as added stiffness and damping from moving water. These parameters affect the natural frequency and damping of a structure, which in the end will affect what vibrations magnitudes the runner will be subjected to for a given frequency of excitation. The behavior of these parameters have recently been investigated by several researchers, but the effect of neighboring blades is yet not understood.

A multi-blade cascade has been tested for four of its different modes of vibration. The results indicate that the slope of the damping with respect to the inverse Strouhal number is constant. This slope was found to be the same as for several single-blade tested performed, both in the same rig and in other works. The implication is that the product of added mass and mode shape does not change significantly.

## 1. Introduction

Evaluating the dynamic response of a Francis runner is becoming increasingly important, in order to avoid resonance with pressure pulsations induced by Rotor-Stator Interactions (RSI). In fact, resonance with RSI has been the cause of failure in several high head Francis runners in the past 15 years [1]. At the design stage, turbine designers need to analyze the levels of vibration a runner is expected to experience during operation, and in order to achieve this, a better understanding of the vibrating system that the runner and water comprises is needed.

A classic damped vibrating system with a single degree of freedom can be characterized by three key parameters: stiffness, mass and damping. If one considered the oscillating turbine blade as a such a system, these characteristics will be slightly modified, as the presence of flowing water adds to stiffness, mass and damping. These parameters have been extensively investigated, and the impact of added mass is well understood [2–5]. The effect on damping has received less attention in the past, but recent studies have been conducted, indicating that the damping is

indeed affected by the moving water. The damping is a critical quantity to understand, as the vibration amplitude is sensitive to damping at resonance. Recent papers have investigated the effect of water velocity on damping, and the general conclusion is that the damping increases with increasing water velocity. [2–4, 6] There is some indication that the damping and natural frequency undergo a change in the lock-in region [4, 6], and Computational Fluid Dynamics (CFD) results indicate that the damping increases linearly up to at least 45 m/s [7]. There are two key limitations with the investigations performed up to this point: They do not evaluate the effect of adjacent blades, and they only investigate a single mode of vibration. The aim of this paper is therefore to investigate the effect of the neighbouring blades, and to state whether or not it is sufficient to examine a single blade. Multiple modes of vibration of a multi-blade cascade will be evaluated, and comparisons will be made to similar works in the field.

## 2. Materials and Methods

The experimental setup and data analysis methods are described in the following section.

### *2.1. Experimental Setup*

The experiments were conducted at the Waterpower Laboratory at the Norwegian University of Science and Technology (NTNU). The test set-up consisted of a 150 mm by 150 mm square channel, containing the hydrofoil in a fixed-beam configuration, i.e. fastened in both ends. The test rig itself is rigid, with steel walls of 25mm thickness. This was done to minimize simulation errors resulting from the assumption of stiff walls.

The hydrofoil geometry is presented in Figure 1. The three hydrofoils are identical, and their centerlines are spaced 39 mm apart.

Blade 1 and 3 were excited to vibration using Piezoelectric Macrofiber Composites (MFCs). MFCs were chosen for their ability to excite vibration with direct frequency- and phase control, making them ideal for this test case. The use of MFCs in hydrofoil testing has been documented previously by Presas et al [9], and they have been successfully employed for hydrofoil experiments by multiple researchers [2–4, 6, 10, 11]. The response was measured with semiconductor strain gauges from Kulite at both the leading edge and the trailing edge, in order to be able to separate the vibration modes of a single blade. The tests were performed in cavitation-free conditions, for velocities up to 20 m/s.

### *2.2. Testing procedure*

*2.2.1. Mode shapes, damping and natural frequencies* Preliminary simulations indicated that the system contains modes with blade 2 as a node. In order to be able to investigate modes, both with blade 2 moving and with blade 2 as a node, a preliminary measurement was performed with excitation at blade 3 only, in stationary water. The Frequency Response Functions (FRFs) from that sweep are shown in Figure 2.

The relative phase delay between the trailing edges and leading edges, along with the natural frequency, are used to identify the modes. The modes chosen for further investigation are shown in Figure 3, and outlined in Figure 2 as vertical dash-dot lines.

In order to get a more powerful response from the system, excitation was applied at both blade 1 and 3 simultaneously. M1, M2 and M3 are achieved by exciting blade 1 and 3 in phase, while M4 is achieved by exciting blade 1 and blade 3 with a phase delay of 180°.

For each water velocity, a preliminary continuous sweep was conducted to roughly locate the frequencies of the modes of interest. The modes were then further investigated using a classical *stepped-sine excitation*, as recommended by Ewins [12]. Each stepped-sine excitation was repeated 30 times to get statistical data to accurately calculate the damping and natural frequency for each mode.

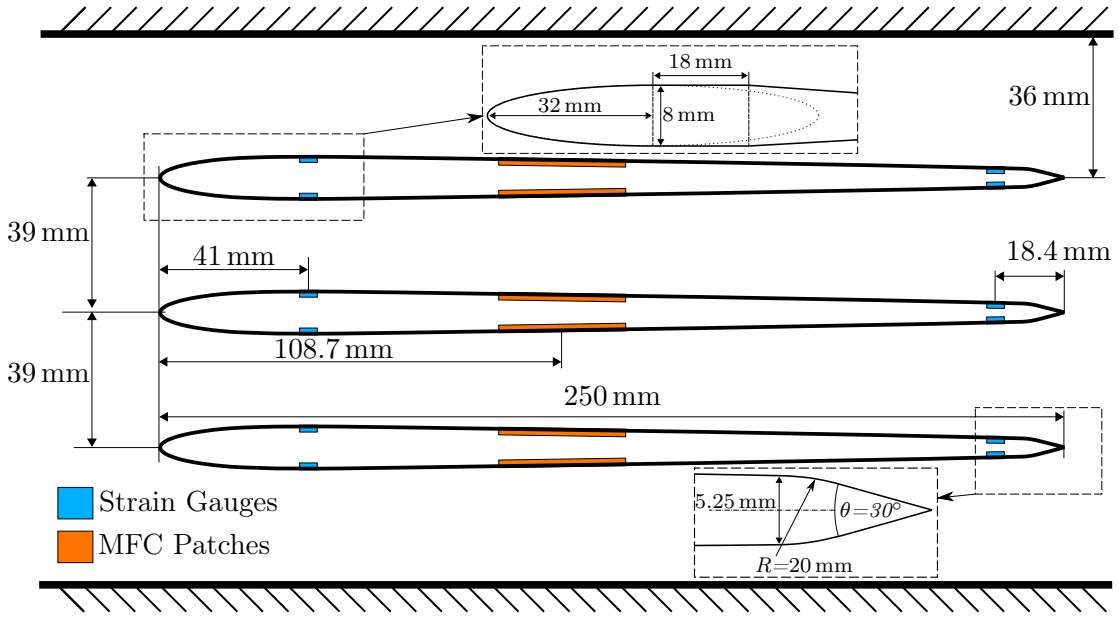


Figure 1: Blade cascade geometry. Note that the trailing edge is symmetric, and that there is a tapering of the hydrofoil, indicated in the detailed image of the leading edge. The choice in leading edge and trailing edge geometries is based on the setup previously employed in the same rig, with a single-blade configuration. [8]. The blade thickness has been reduced to 18mm, to counterbalance the increased "blocked area" imposed by multiple blades. The strain gauges were placed as close to the leading and trailing edges as possible while being situated in a flat area of the geometry, for practical reasons. The MFC placement was dictated by a minimum distance to the hydrofoil's center-line

*2.2.2. Analysis* The amplitudes of both the excitation and response were calculated using the Welch method as implemented by MATLAB. The Welch method is an estimate of the power spectrum, which reduces the noise by reducing the frequency resolution through overlapping windows. For the amplitude estimates, the flattop window was chosen, with 30 windows overlapping by 50%. The sample rate was 5120 S/s, and the measurement length was 14 000 samples. Since the Welch method in MATLAB does not yield phase data, the phase difference between the excitation and response was estimated by calculating the cross-power spectral density. The magnitude ratio between the excitation and response, along with the phase difference was used to recreate the complex FRF, which was used to calculate damping and natural frequency, using the Nyquist diagram. By plotting the real part vs. the imaginary part of the FRF, a resonant region will appear as a circle. By curve fitting the data to a circle, geometric properties of the curve fit can be used to accurately estimate modal properties. This method was chosen, since it does not rely on data far away from the resonant region, and is therefore less sensitive to neighbouring modes of vibration. For a detailed explanation of the circle-fit method and the Nyquist diagram, the reader is referred to Ewins [12], Craig and Kurdila [13], and Bergan et al [6].

## 3. Results and discussion

The resulting variations in damping are shown in Figure 4

Due to the low amplitude of vortex shedding, measurements without external excitation were unable to determine the velocity for lock-in. However, since the hydrofoil geometry is quite

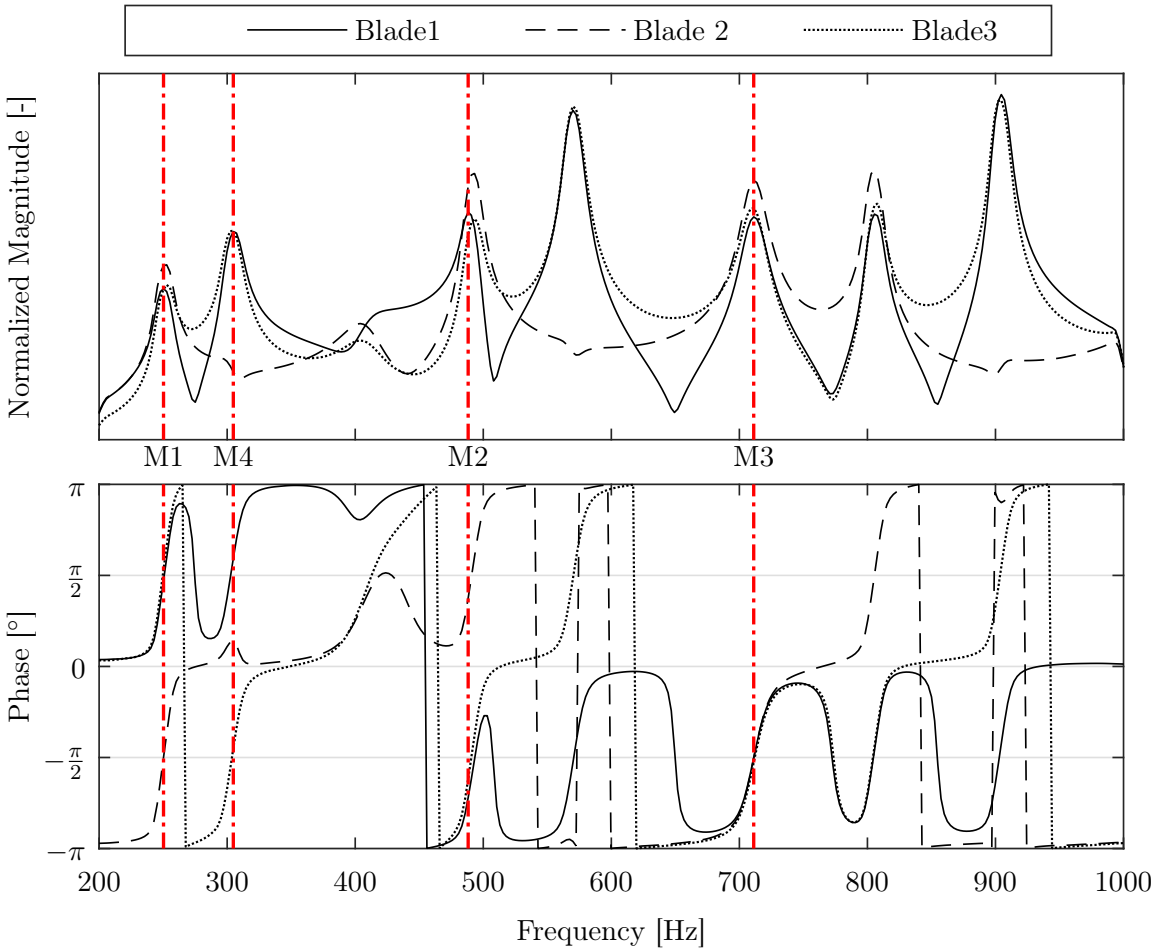


Figure 2: Bode plot for excitation at a single blade. The vertical dash-dot lines indicate the frequency of the modes investigated. Note that this is a preliminary and transient measurement, as such, the exact amplitudes of each mode is not accurate. This can be seen in particular for the amplitude of blade 2 around 310 Hz, 575 Hz, and 900 Hz. These are frequencies where blade 2 is a node, but in this transient measurement, the anti-resonance is swept through before blade 2 reaches zero amplitude. The bottom plot shows the phase delay between each blade and the excitation signal. Note that only trailing edge measurements are shown here.

similar to previous investigations in the same rig [8], the lock-in velocity is expected to be found at more or less the same velocity. Referring to Figure 4, it is evident that a change in the slope of the damping factor occurs at around 5 to 10 m/s, depending on which mode is investigated. This is due to the difference in natural frequency for the different vibrational modes, causing lock-in to occur at different velocities. According to Figure 4, we expect lock-in to occur in the order M1, M4, M2, M3. This corresponds to increasing natural frequency, see Figure 3.

Another interesting feature of Figure 4, is that M3 appears to have a much flatter slope than all the other modes. In order to make comparisons between the different modes, the reduced velocity is suggested as a dimensionless term. The reduced velocity is defined as the ratio between the time for a single vibration cycle, and the time for a particle to travel from the leading edge to the trailing edge. The formula is given in Equation (1)

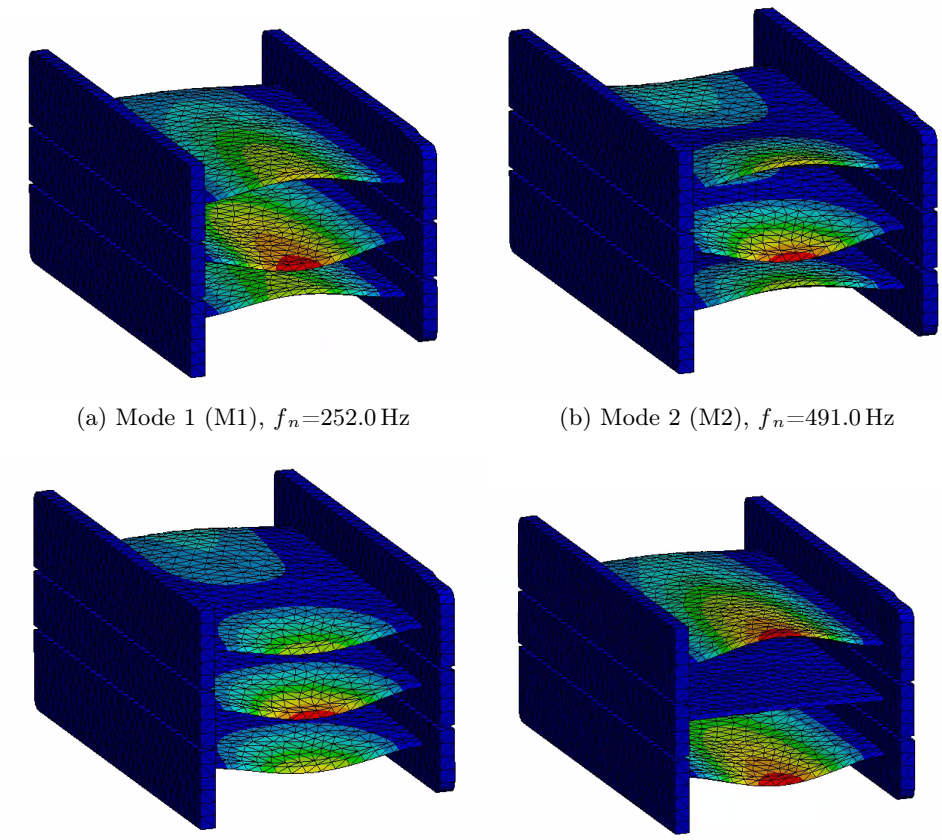

(a) Mode 1 (M1), $f_n$=252.0 Hz (b) Mode 2 (M2), $f_n$=491.0 Hz

(c) Mode 3 (M3), $f_n$=708.2 Hz (d) Mode 4 (M4), $f_n$=300.1 Hz

Figure 3: The four modes investigated. Note that the main difference between M1 and M2 is the phase between the leading and trailing edge. Also note that for M4, the middle blade is stationary.

$$v^* = \frac{v}{L \cdot f_n} \tag{1}$$

The reduced velocity is, in fact, the inverse of the Strouhal number, defined in Equation (2), but with the chord length in stead of the trailing edge thickness as the characteristic length.

$$St = \frac{fL}{v} \tag{2}$$

in Equation (2), $St$ is the Strouhal number, $f$ is the frequency, $L$ is the "characteristic length", and $v$ is the velocity.

If the results from Figure 4 are plotted against the inverse Strouhal number, the behavior of the different modes is much more similar, see Figure 5

Figure 5 shows that, for this particular test rig, the damping factor evolution is more or less the same for all the tested modes of vibration, when plotted against the inverse Strouhal number. This is an interesting result, indicating that some generalizations can be made. For comparison purposes, the experimental data of Coutu et al [2] has been manually read from the plot shown in Figure 6. Lacking information about the physical scales, the unit length has been omitted in the modified reduced velocity used in the comparison. This does not affect the internal similitude

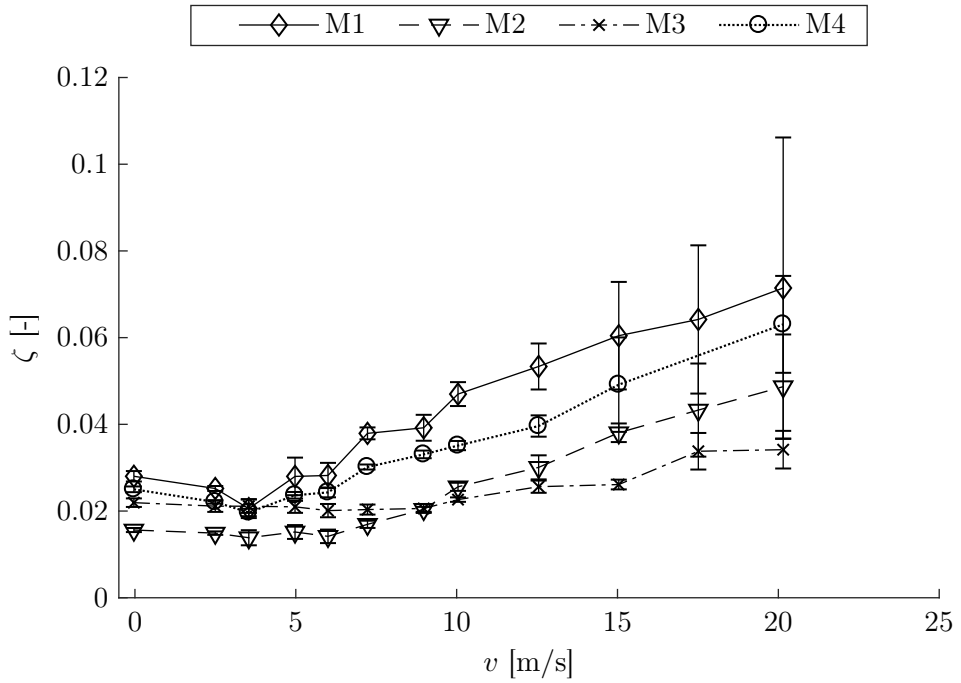


Figure 4: Damping vs velocity for the four modes investigated. Note that M3 deviates from the common pattern of the other modes, maintaining a nearly constant damping.

between the modes investigated in this paper, as the geometry, and hence the unit length, is unchanged throughout the experiment.

Figure 7 shows the damping plotted against the modified reduced velocity, defined by Equation (3)

$$v^{**} = \frac{v}{f_n} \tag{3}$$

As Figure 7 shows, the slopes for H0, H1 and H3 share the same similarity as before, but in the lower left corner of the graph, it is evident that the data obtained in this paper, combined with previous measurements in the same test rig [6–8], approximate the same slope. This is clearer when considering Figure 8, where the data for $v^{**} < 0.08$ is displayed.

The similarity in slope means that the actual damping of low-frequency vibrations increases at a higher rate than those of high-frequency vibration. However, this assertion is based on measurements performed at a limited selection of natural frequencies, and more data is needed for making an empirical generalization. In addition, this limitation in $v^{**}$ investigated leaves some uncertainty to the slope, as Figure 8 shows, where the markers for F0 and M2 apparently follow a steeper curve. Nonetheless, not only do similar hydrofoil in the same rig approximate the same slope, different modes of a multi-bladed cascade approximate the same slope, as well as experiments performed in an entirely different test rig, with natural frequency an order of magnitude lower. As a simple test of this concept, CFD simulations were performed on one of the hydrofoils previously investigated in this test rig, denoted F1 in Figure 7. For details about the CFD setup, see Tengs et al [7]. The modified reduced velocity was altered by manually altering the hydrofoil's natural frequency in the numerical setup. The results of this simulation are shown in Figure 7.

If one were to interpret the physical meaning of the modified reduced velocity, $\frac{1}{f_n}$ is a measure

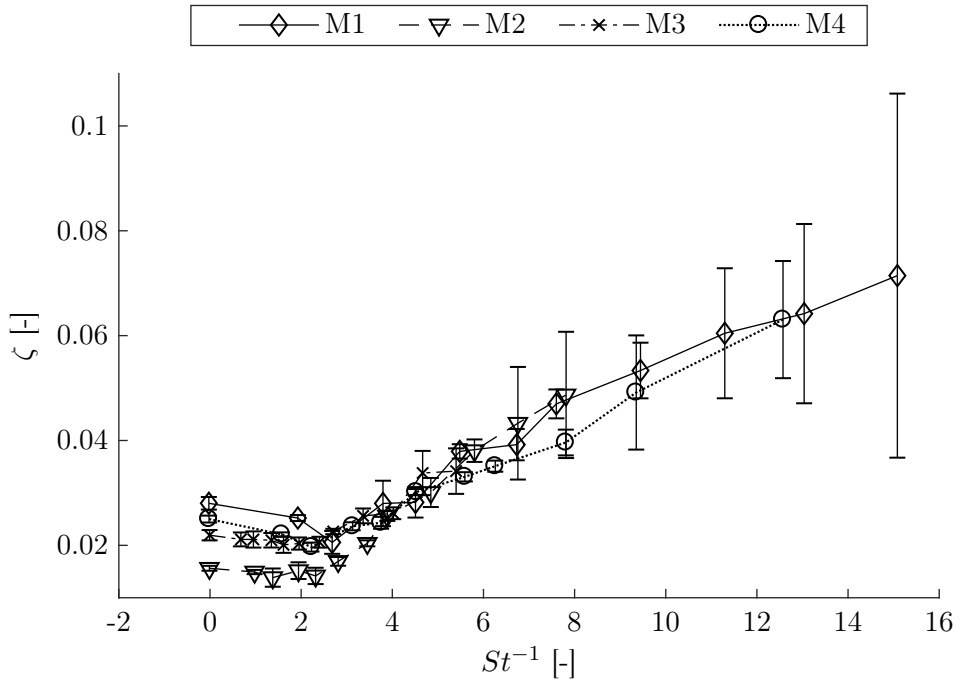


Figure 5: Damping plotted against the inverse Strouhal number. Note that all modes of vibration show a change in behavior around $St^{-1} = 2.5$. This is the lock-in region as discussed in Figure 4, meaning that the vortex shedding frequency is equal to the natural frequency. The relatively high value for $St$ at lock-in indicates that the trailing edge thickness is not representative for the wake thickness for this geometry.

of time, namely the time per cycle of vibration, and $v$ is a measure of how much water passes the blade per unit time. In that regard, $v^{**}$ is a measure of how much water passes the trailing edge per cycle of vibration, and could very well be a relevant quantity in determining the effect of the water's momentum on the trailing edge's vibration. Going back to the reduced velocity, or the inverse Strouhal number, the selection of the characteristic length is not straightforward. For simple geometries, there are conventions, such as for the cylinder, the diameter is the characteristic length. For a hydrofoil, the chord length is a viable candidate, and it has been used by Yao [4]. The blade thickness is also a possibility, which in combination with trailing edge geometry is widely used for estimating vortex shedding frequencies [14]. Looking back at the damping comparisons, Figures 7 and 8, it is evident that for the vibrations investigated, it doesn't really matter. The slope is more or less the same, but that is not surprising. Although the test rigs, natural frequencies, number of blades, and physical scales are different, the mode shape of each single blade is not that different in each case. For a broader investigation on how damping behaves in submerged structures, with different boundary conditions and other modes of vibration, there is a need to asses geometric parameters. This is where the use of characteristic length is a drawback: it does not factor in how much of the structure is vibrating.

At this point, it is appropriate to take a step back, and consider the theoretical work performed by Monette et al [10]. The damping ratio for a submerged vibrating structure can be calculated as follows:

$$\zeta = \frac{v}{f_n}\left[1 - \left(\frac{f_n}{f_v}\right)^2\right] \frac{\iint \Phi(x,y)\frac{\partial \Phi(x,y)}{\partial x}\,dx\,dy}{\iint \Phi^2(x,y)\,dx\,dy} \tag{4}$$

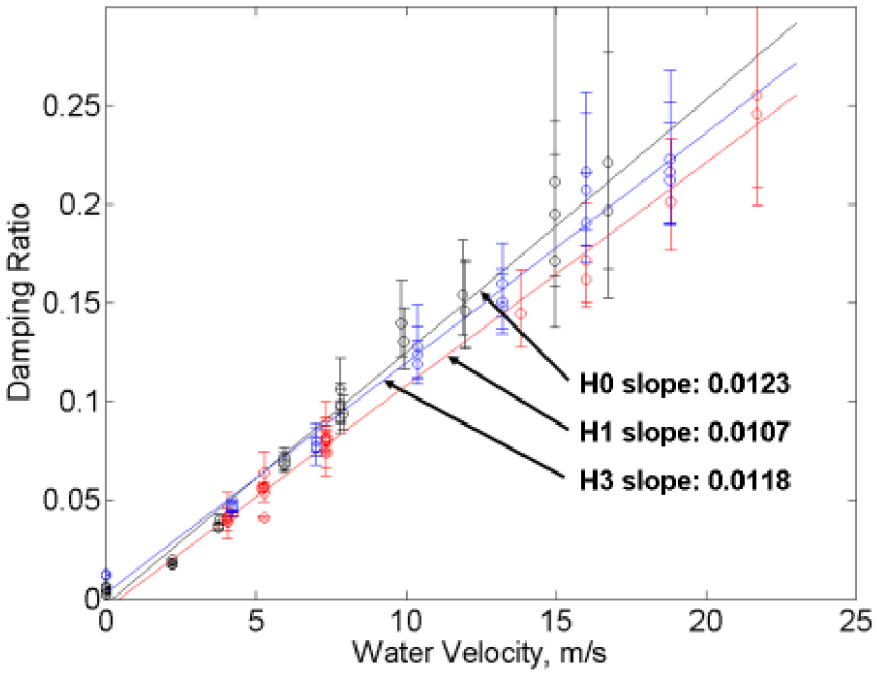


Figure 6: Damping measurements obtained by Coutu et al [2]

In Equation (4), $f_n$ denotes the structure's natural frequency in the fluid, $f_v$ the natural frequency in vacuum, while $\Phi$ denotes the mode shape, an integral of the structure's deflection.

By considering the equation, it is clear that it contains three main parts:

(i) the "modified reduced velocity", as defined in Equation (3)

(ii) a measure of the added mass, or the thickness of fluid affected by the motion, defined by

$$\widehat{M} = \left[1 - \left(\frac{f_n}{f_v}\right)^2\right] \tag{5}$$

(iii) a measure of the "amount of movement" of the structure, namely the mode shape.

$$\widehat{\Phi} = \frac{\iint \Phi(x,y) \frac{\partial \Phi(x,y)}{\partial x}\, dx\, dy}{\iint \Phi^2(x,y)\, dx\, dy} \tag{6}$$

If only the results measured in this experimental campaign are considered, the slope of damping ratio is constant above lock-in velocities, meaning that the second and third term in Equation (4) must either cancel each other out, or individually remain constant for the different mode shapes.

$$\widehat{M}\widehat{\Phi} = const \tag{7}$$

It is not unreasonable to expect the mode shape integral to yield the same result for different hydrofoils, given that the boundary conditions are similar, ie. fixed beam, single blade. Given that the vibration deflections are not too large, the relative added mass is not expected to change, and as such, Equation (7) still holds: the product is constant, and hence the damping slope is

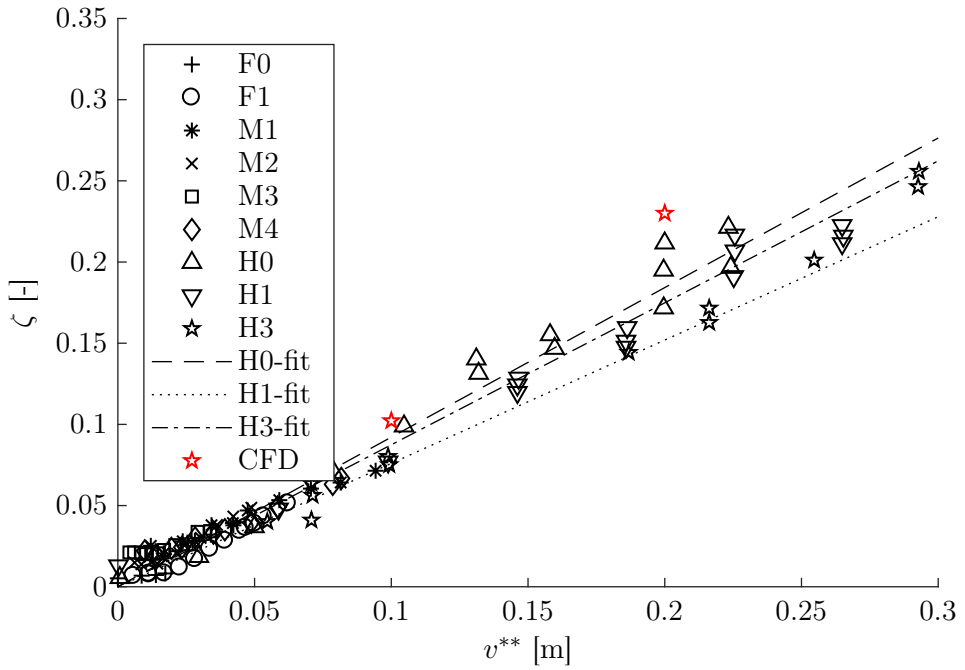


Figure 7: Damping comparison. The lines indicate the linear curve fits from Figure 6, when corrected for their natural frequencies. The mean slope of all the plots was found to be $\zeta/v^{**} = 0.873$

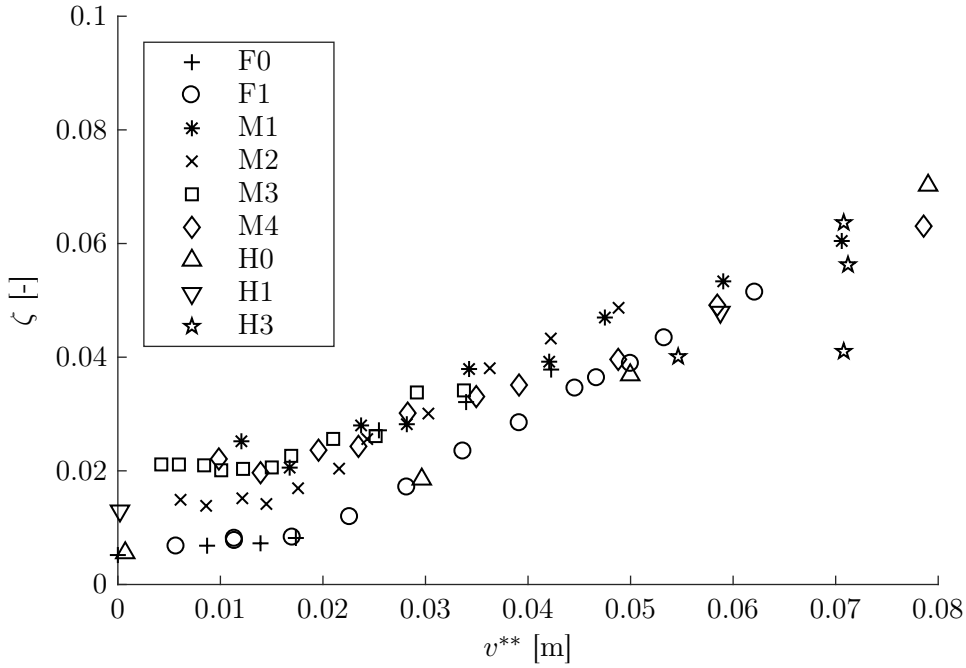


Figure 8: Damping comparison zoomed.

constant. In fact, small variations in the added mass, $\widehat{M}$, could explain the difference in the slope in Coutu's measurements, see Figure 6.

Even for the three-bladed cascade, although the blade movement is coupled through the water, their deflections can still be integrated in Equation (6), yielding a similar value as for their single-blade counterpart. The value of $\widehat{M}$ is a bit more tricky to estimate for the three bladed cascade case. This is because the response of the water does more than just add mass and damping, it couples the structural movement, producing modes that were not there in air. As such, the assumption of unchanged modes does not hold in a strict sense, but one could speculate that the relatively large spacing of the hydrofoils, combined with the relatively high frequency of vibration, means that the relative added mass of each blade is not affected by the proximity o neighbouring blades. As such, the damping should still adhere to Equation (4), with some substitutions for the estimate for added mass.

This raises an interesting possibility: Even with a multi-blade cascade, with blades coupled through the fluid, we still expect the damping to be described by Equation (4), as long as the appropriate term is found to describe the amount of added mass. If this is indeed true for larger and more complex structures, a runner may be analyzed by considering it as a collection of blades with individually known modes of vibration. However, there are still some unknown parameters to this: Although this experiment shows that three blades behave similarly as one, it is not known for certain if that behavior will translate to a cascade of more blades. Additionally, the question of complex modes and rotational symmetry is not assessed in this experiment, and it is therefore not known if the damping estimates for such a vibration will be different.

## 4. Conclusion

This experiment indicates that the modes of vibration in a blade cascade show the same behavior in damping when plotted against the reduced velocity. Further comparisons with other experiments indicate that the damping slope can be determined if the natural frequency of the hydrofoil is known, for blades with the same boundary conditions. This can be described by theory developed by Monette et al, and the present investigations show that the product of the added mass and the mode shape integral remain fairly constant for fixed-beam hydrofoils. Moreover, it has also been shown that this product is unchanged when higher modes of multi-blade cascades are considered. This indicates that damping estimates for the blades of a turbine runner can be performed in the same way as for a single blade. However, this has only been demonstrated on a structure exhibiting real modes of vibration. Four modes of vibration were tested, including one where the center blade was stationary. The observed behavior is that the damping factor is unchanged up to $St^{-1} = 2.5$, beyond which the change is linear with respect to reduced velocity. The slope was the same for all modes of vibration, when plotted as reduced values, $\zeta/v^{**} = 0.873$.

## 5. Further Work

The main focus of further investigations should be to systematically vary different geometric parameters, in order to provide data for the added mass and the mode shape integral for typical geometries. In addition, further work on such a multi-blade cascade should aim to investigate the effect of complex modes. Complex modes are not necessarily going to behave similarly to real vibration modes, and this investigation is of particular relevance for turbines, as they are prone to complex modes due to their rotational symmetry. In addition, although several modes of vibration have been investigated in this work, they are quite similar in their shape. For further investigations on the turbine blade behaviour in high-velocity flows, a twisted blade is suggested, as it is expected to produce less symmetric vibrational modes. Finally, the effects of vibration amplitude have not been investigated in this work. At large amplitudes, the added mass might begin tho change, altering the slope of the damping.

## 6. Acknowledgements
The research was carried out as a part of HiFrancis, a high-head Francis turbine research program supported by the Norwegian Research Council, The Norwegian Hydropower industry, and the Norwegian Center for Hydropower.

## Nomenclature
### Greek Symbols
| | |
|---|---|
| $\Phi$ | Mode shape |
| $\phi$ | Taper angle |
| $\theta$ | Trailing edge angle |
| $\widehat{\Phi}$ | Measure of mode shape movement |
| $\zeta$ | Damping |

### Latin Symbols
| | |
|---|---|
| $\widehat{M}$ | Measure of added mass |
| $f$ | Frequency |
| $L$ | Cord Length |
| $St$ | Strouhal number |
| $v$ | Water velocity |
| F0 | Old Hydrofoil |
| F1 | New Hydrofoil |

### Indices, superscripts
| | |
|---|---|
| $**$ | Reduced Modified |
| $*$ | Reduced |

### Indices, subscripts
| | |
|---|---|
| $n$ | Natural |
| $v$ | In vacuum |

## References

[1] Østby P T K, Billdal J T, Sivertsen K, Haugen B and Dahlhaug O G 2016 *International journal on hydropower and dams*
[2] Coutu A, Seeley C, Monette C, Nennemann B and Marmont H 2012 *IOP Conference Series: Earth and Environmental Science*
[3] Roth S, Calmon M, Farhat M, Münch C, Bjoern H and Avellan F 2009 *Proceedings of the 3rd IAHR International Meeting of the Workgroup on Cavitation and Dynamic Problems in Hydraulic Machinery and Systems* vol 1 (Brno, Czech Republic: Brno University of Technology)
[4] Yao Z, Wang F, Dreyer M and Farhat M 2014 *Journal of Fluids and Structures*
[5] Reese M C 2010 *Vibration and Damping of Hydrofoils in Uniform Flow* Master's thesis
[6] Bergan C W, Solemslie B W, Østby P and Dahlhaug O G 2018 *International Journal of Fluid Machinery and Systems*
[7] Tengs E O, Bergan C W, Jakobsen K R and Storli P T 2018 *IOP Conference Series: Earth and Environmental Science*
[8] Bergan C W, Tengs E O, Solemslie B W and Dahlhaug O G 2018 *IOP Conference Series: Earth and Environmental Science*
[9] Presas A, Valentin D, Egusquiza E, Valero C, Egusquiza M and Bossio M 2016 *Proceedings*
[10] Monette C, Nennemann B, Seeley C, Coutu A and Marmont H 2014 *IOP Conference Series: Earth and Environmental Science*
[11] Seeley C, Coutu A, Monette C, Nennemann B and Marmont H 2012 *Smart Materials and Structures*
[12] Ewins D J 2000 *Modal Testing: Theory, Practice, and Application* 2nd ed (*Mechanical engineering research studies* no 10) (Baldock, Hertfordshire, England ; Philadelphia, PA: Research Studies Press)
[13] Craig R R, Kurdila A and Craig R R 2006 *Fundamentals of Structural Dynamics* 2nd ed (Hoboken, N.J: John Wiley)
[14] Heskestad G and Olberts D R 1960 *Journal of Engineering for Power*